Odd nuclei and quasiparticle excitations within the Barcelona Catania Paris Madrid energy density functional

S. A. Giuliani [1,2,*] and L. M. Robledo [1,3,†]

[1]*Departamento de Física Teórica and CIAFF, Universidad Autónoma de Madrid, E-28049 Madrid, Spain*

[2]*Department of Physics, Faculty of Engineering and Physical Sciences, University of Surrey, Guildford, Surrey GU2 7XH, United Kingdom*

[3]*Center for Computational Simulation, Universidad Politécnica de Madrid, Campus de Montegancedo, Bohadilla del Monte, E-28660-Madrid, Spain*

An extension of the Barcelona Catania Paris Madrid (BCPM) energy density functional is proposed to deal with odd-mass systems as well as multiquasiparticle excitations. The extension is based on the assumption that the equal filling approximation (EFA) is a valid alternative to the traditional full blocking procedure of the Hartree-Fock-Bogoliubov method. The assumption is supported by the excellent agreement between full blocking and EFA calculations obtained with different parametrizations of the Gogny interaction. The EFA augmented BCPM functional is used to compute low energy excitation spectra of selected nuclei in different regions of the nuclear chart, and high-K isomers in ^{178}Hf. We show that BCPM predictions are in good agreement with Gogny D1M results and experimental data.

I. INTRODUCTION

Nuclei with an odd number of protons or neutrons are an archetypical example of spin-polarized fermionic systems. Due to the presence of an unpaired nucleon, their theoretical description using mean-field models poses additional challenges compared to even-even systems. This is because the short-range nature of pairing interaction couples the nucleons in Cooper pairs in order to maximize their spatial overlap, simplifying the description of nuclei with an even number of protons and neutrons. Conversely, odd-A nuclei break time-reversal symmetry, hence removing Kramers degeneracy in single-particle levels and requiring the inclusion of energy density functional (EDF) time-odd fields. This results in an increased computational cost, which has traditionally limited the number of calculations devoted to odd-A nuclei as well as EDFs employed in such studies [1–18].

The Barcelona Catania Paris Madrid (BCPM) energy density functional [19] represents a fruitful alternative to more traditional phenomenological approaches like the Skyrme or Gogny family of forces. It delivers low energy nuclear structure results for even-even nuclei of the same quality as those obtained with the well-known Gogny D1M. The relatively low computational effort required by mean field calculations with BCPM has fostered a number of applications of BCPM, including large-scale calculations of finite nuclei properties [20,21] and applications to r-process nucleosynthesis

calculations [22] and neutron star physics [23] (see [24] for a recent review on BCPM). However, time-odd fields are not considered in the functional, preventing the description of odd-mass systems as well as single-particle excitations using the traditional blocking method of the Hartree-Fock-Bogoliubov (HFB) method. BCPM is built on polynomial fits to realistic nuclear matter equations of state for symmetric and pure neutron systems given as a function of the density. The same polynomial form is used to define an energy density functional for finite nuclei just by replacing the nuclear matter density with the density of finite nuclei. A Gaussian potential is introduced in the direct channel to simulate surface effects and, finally, the traditional zero-range spin-orbit plus Coulomb potentials are added to define the particle-hole component of the functional. A density-dependent pairing term [25] completes the functional. In the original formulation of BCPM, polarization effects at the nuclear matter level were not considered and, therefore, the functional is only valid for time-reversal symmetry-preserving physical cases, such as the ground state of even-even nuclei. This limitation prevents the use of BCPM to describe properties of odd-A and odd-odd nuclei as well as multiquasiparticle excitations by means of the traditional HFB blocking method. On the other hand, by comparing different theoretical approaches describing odd-A nuclei [12], it has been argued that the time-reversal symmetry-preserving equal filling approximation (EFA) [8] is a valid approximation to full quasiparticle blocking. This empirical conclusion is based on calculations using zero-range Skyrme forces and therefore its range of validity is somehow limited. The main effect of blocking is to quench pairing correlations, reducing thereby the pairing gap

*samuel.giuliani@uam.es
†luis.robledo@uam.es

and the typical excitation energy of one-quasiparticle states. The EFA leads to the same quenching of pairing correlations even at the quantitative level. On the other hand, the EFA can be viewed as a full blocking calculation in which time-odd fields in the Hartree-Fock and pairing fields generated by the unpaired nucleon are neglected [12]. The good performance of the EFA in describing odd-A nuclei with Skyrme forces, and the absence of time-odd fields in its formulation, suggests that EFA could be used to extend the realm of the BCPM functional to describe odd-A nuclei and quasiparticle excitations. The motivation for this paper is threefold: First, we show how the approximate equivalence between EFA and full blocking is also valid with Gogny forces, in order to reinforce the empirical conclusion extracted from Skyrme calculations [12]. Second, we show how to implement multiquasiparticle excitation in the standard variational EFA framework. Finally, we assess the accuracy of BCPM-EFA predictions by comparing against both Gogny D1M predictions and experimental data of spin and parity of ground and low-lying excited states, in a set of selected nuclei scattered across the nuclear chart. Multiquasiparticle excitations are also considered in the paradigmatic case of high-K isomeric states in ^{178}Hf.

The paper is organized as follows. The theoretical EFA framework and the BCPM interaction are outlined in Sec. II. Section III is devoted to a comparison between full blocking and EFA calculations. In Sec. IV, the EFA results of low-energy spectra and high-K states are presented. Conclusions and perspectives for future studies are summarized in Sec. V.

II. THEORETICAL METHODOLOGY

The self-consistent mean field description of odd-A nuclei, as well as that of multiquasiparticle excitation, is based on the HFB method with blocking. In the standard HFB method [26], the concept of quasiparticle is introduced by means of the Bogoliubov transformation

$$\begin{pmatrix} \beta \\ \beta^\dagger \end{pmatrix} = \begin{pmatrix} U^\dagger & V^\dagger \\ V^T & U^T \end{pmatrix} \begin{pmatrix} c \\ c^\dagger \end{pmatrix} \equiv W^+ \begin{pmatrix} c \\ c^\dagger \end{pmatrix}. \tag{1}$$

The associated HFB state $|\Phi\rangle$ is defined as the vacuum state for all the annihilation quasiparticle operators β_μ, i.e., $\beta_\mu|\Phi\rangle = 0$ for labels μ indexing all the quasiparticle configurations. An important concept in the HFB theory is "number parity", which is nothing but the parity (even or odd) of the number of particles in $|\Phi\rangle$ and its excitations. Number parity is a symmetry of the system, and wave functions with opposite values cannot be mixed together. An even-even nucleus has to be described by a HFB state with even number parity for both protons and neutrons. The quasiparticle operators carry number parity 1 and therefore $\beta_\mu^\dagger|\Phi\rangle$ has opposite number parity to that of $|\Phi\rangle$. Therefore, genuine excitations of a given system $|\Phi\rangle$ are given by two, four, etc. quasiparticle excitations whereas one, three, etc. quasiparticle excitations correspond to a neighbor odd-mass system if $|\Phi\rangle$ contains an even number of particles (and vice versa). As a consequence, odd-A nuclei have to be treated with a "blocked" wave function $\beta_{\mu_B}^\dagger|\Phi\rangle$ breaking time-reversal invariance because of its dependence on the quantum number μ_B.

For fully paired configurations $|\Phi\rangle$ (i.e., no blocking), Bogoliubov amplitudes U and V are determined by using the variational principle on the HFB energy $E_{\text{HFB}} = \langle\Phi|\hat{H}|\Phi\rangle$ leading to the well know HFB equation (see [26] for a gentle description of the HFB method). Conversely, the U and V for a blocked state are obtained by minimizing $E_{\text{HFB}}^{(\mu_B)} = \langle\Phi|\beta_{\mu_B}\hat{H}\beta_{\mu_B}^\dagger|\Phi\rangle$. The blocking procedure introduces an additional level of complexity in the minimization process due to the dependence of the energy on μ_B. One must consider the variational principle for U and V considering all possible values of the quantum numbers μ_B of the blocked levels and choosing for the ground state the value of μ_B leading to the lowest energy. Taking into account that $E_{\text{HFB}}^{(\mu_B)} = \langle\Phi|\hat{H}|\Phi\rangle + E_{\mu_B} + \cdots$, where E_{μ_B} is the quasiparticle energy of level μ_B and the ellipses represent residual interaction corrections, one can expect that a search limited to those blocking quasiparticles $\beta_{\mu_B}^\dagger$ with small values of the quasiparticle energies E_μ will end up in the lowest energy solution. Typically, considering the ten lowest quasiparticle energies leads with confidence to the ground state of the odd-A system. On the other hand, the advantage of the above procedure is that one obtains not only the ground state but also the lowest energy single-particle spectrum.

Wick's theorem also holds for blocked HFB states, and therefore the blocked energy $E_{\text{HFB}}^{(\mu_B)} = \langle\Phi|\beta_{\mu_B}\hat{H}\beta_{\mu_B}^\dagger|\Phi\rangle$ can be expressed in the usual form in terms of the blocked density matrix ρ^{μ_B} and pairing tensor κ^{μ_B} given by

$$\rho_{kk'}^{(\mu_B)} = \langle\Phi|\beta_{\mu_B}c_{k'}^\dagger c_k\beta_{\mu_B}^\dagger|\Phi\rangle$$
$$= (V^*V^T)_{kk'} + \left(U_{k'\mu_B}^*U_{k\mu_B} - V_{k'\mu_B}^*V_{k\mu_B}^*\right) \tag{2}$$

and

$$\kappa_{kk'}^{(\mu_B)} = \langle\Phi|\beta_{\mu_B}c_{k'}c_k\beta_{\mu_B}^\dagger|\Phi\rangle$$
$$= (V^*U^T)_{kk'} + \left(U_{k\mu_B}V_{k'\mu_B}^* - U_{k'\mu_B}V_{k\mu_B}^*\right). \tag{3}$$

Owing to their dependence on the quantum number μ_B, these two matrices are not time-reversal invariant. In order to restore time-reversal symmetry, the EFA [8] postulates the use of the "averaged" density

$$\rho_{kk'}^{\text{EFA}} = (V^*V^T)_{kk'} + \tfrac{1}{2}\left(U_{k'\mu_B}U_{k\mu_B}^* - V_{k'\mu_B}^*V_{k\mu_B}\right.$$
$$\left. + U_{k'\overline{\mu}_B}U_{k\overline{\mu}_B}^* - V_{k'\overline{\mu}_B}^*V_{k\overline{\mu}_B}\right) \tag{4}$$

and "average" pairing tensor

$$\kappa_{kk'}^{\text{EFA}} = (V^*U^T)_{kk'} + \tfrac{1}{2}\left(U_{k\mu_B}V_{k'\mu_B}^* - U_{k'\mu_B}V_{k\mu_B}^*\right.$$
$$\left. + U_{k\overline{\mu}_B}V_{k'\overline{\mu}_B}^* - U_{k'\overline{\mu}_B}V_{k\overline{\mu}_B}^*\right) \tag{5}$$

instead. The EFA energy is obtained by replacing $\rho_{kk'}^{(\mu_B)}$ and $\kappa_{kk'}^{(\mu_B)}$ with their EFA equivalents in the expression of the blocked energy $E_{\text{HFB}}^{(\mu_B)}$. It was shown in Ref. [8] that this procedure can be justified by using quantum statistical mechanic concepts. The EFA corresponds to a statistical admixture of the states $\beta_{\mu_B}^\dagger|\Phi\rangle$ and $\beta_{\overline{\mu}_B}^\dagger|\Phi\rangle$ with equal probability 1/2. Traditionally, quantum statistical admixtures are better described by using a density matrix operator given by the statistical ensemble considered. However, arbitrary statistical distributions can also be handled by introducing a density matrix operator

$\hat{\mathcal{D}}$ chosen in such a way that $\hat{\mathcal{D}}|\Phi\rangle = |\Phi\rangle$ and $\hat{\mathcal{D}}\beta_\mu^\dagger = p_\mu \beta_\mu^\dagger \hat{\mathcal{D}}$, p_μ being the probability of the one-quasiparticle excitation $\beta_\mu^\dagger|\Phi\rangle$ [8]. In this formalism, the statistical mean value of an arbitrary operator is given by

$$\langle\hat{O}\rangle_S = \frac{\text{Tr}[\hat{O}\hat{\mathcal{D}}]}{\text{Tr}[\hat{\mathcal{D}}]} = \frac{1}{Z}\Bigg(\langle\Phi|\hat{O}|\Phi\rangle + \sum_\mu p_\mu \langle\Phi|\beta_\mu \hat{O}\beta_\mu^\dagger|\Phi\rangle$$
$$+ \frac{1}{2!}\sum_{\nu\mu} p_\mu p_\nu \langle\Phi|\beta_\mu\beta_\nu \hat{O}\beta_\nu^\dagger\beta_\mu^\dagger|\Phi\rangle \cdots\Bigg) \quad (6)$$

with

$$\text{Tr}[\hat{\mathcal{D}}] = Z = 1 + \sum_\mu p_\mu + \sum_{\nu<\mu} p_\mu p_\nu \cdots = \prod_\mu (1+p_\mu) \quad (7)$$

It is worthwhile to remark that in the statistical framework there are contributions from terms with different number parity. However, it has been shown by using number parity projection techniques that the contamination is not relevant for describing the physics [27–29]. Thanks to the existence of a statistical Wick's theorem (see for instance the proof given by Gaudin [30] or Perez-Martin and Robledo [31] for a more recent account), it is possible to compute any statistical mean value of a product of creation and annihilation operators in terms of the corresponding contractions. Therefore, it is possible to express the statistical mean value of the energy $\langle\hat{H}\rangle_S = \text{Tr}[\hat{H}\hat{\mathcal{D}}]/\text{Tr}[\hat{\mathcal{D}}]$ by using the standard expression

$$\langle\hat{H}\rangle_S = \text{Tr}[t\rho] + \tfrac{1}{2}\text{Tr}[\Gamma\rho] - \tfrac{1}{2}\text{Tr}[\Delta\kappa^*], \quad (8)$$

where Γ is the mean-field potential, Δ the pairing field, and the density matrix and pairing tensor are given by the contractions

$$\rho_{kk'} = \frac{\text{Tr}(c_{k'}^\dagger c_k \hat{\mathcal{D}})}{\text{Tr}(\hat{\mathcal{D}})}, \quad \kappa_{kk'} = \frac{\text{Tr}(c_{k'} c_k \hat{\mathcal{D}})}{\text{Tr}(\hat{\mathcal{D}})}. \quad (9)$$

In the EFA case, the probabilities are given by

$$p_\mu = \begin{cases} 1 & \text{if } \mu = \mu_B \text{ or } \overline{\mu}_B, \\ 0 & \text{otherwise.} \end{cases} \quad (10)$$

Inserting these probabilities into the contractions of Eq. (9) and taking into account the definition of the statistical average Eq. (6), one comes to the conclusion that the probabilities of Eq. (10) lead to the density matrix and pairing tensors of the EFA Eqs. (4) and (5). As a consequence, the statistical average of the energy with the probabilities of Eq. (10) is nothing but the EFA energy

$$E_{\text{EFA}} = \text{Tr}[\hat{H}\hat{\mathcal{D}}^{\text{EFA}}]/\text{Tr}[\hat{\mathcal{D}}^{\text{EFA}}]. \quad (11)$$

This result justifies the otherwise *ad hoc* expression of the EFA energy and provides its interpretation as the statistical mean value of the Hamiltonian taken with the EFA density operator. By using Eq. (6) together with Eq. (10), the EFA energy E_{EFA} can also be written in a more transparent way as

$$E_{\text{EFA}} = \tfrac{1}{4}\big(\langle\Phi|\hat{H}|\Phi\rangle + \langle\Phi|\beta_{\mu_B}\hat{H}\beta_{\mu_B}^\dagger|\Phi\rangle + \langle\Phi|\beta_{\overline{\mu}_B}\hat{H}\beta_{\overline{\mu}_B}^\dagger|\Phi\rangle$$
$$+ \langle\Phi|\beta_{\mu_B}\beta_{\overline{\mu}_B}\hat{H}\beta_{\overline{\mu}_B}^\dagger\beta_{\mu_B}^\dagger|\Phi\rangle\big). \quad (12)$$

This expression shows that the EFA energy is simply an average with equal weights of the energy of the reference

even-even wave function $|\Phi\rangle$, the energies of one-quasiparticle excitations with quantum numbers μ_B and $\overline{\mu}_B$, and the energy of the two-quasiparticle excitation with the same quantum numbers. This result is very illustrative of the nature of the EFA as a statistical theory. The same kind of arguments can be applied to compute mean values of any kind of operators in the EFA framework. An important result that can be easily derived is that the EFA mean values of any one-body operator, which according to the general result can be written as

$$\langle\hat{O}\rangle_{\text{EFA}} = \tfrac{1}{4}\big(\langle\Phi|\hat{O}|\Phi\rangle + \langle\Phi|\alpha_{\mu_B}\hat{O}\alpha_{\mu_B}^\dagger|\Phi\rangle + \langle\Phi|\alpha_{\overline{\mu}_B}\hat{O}\alpha_{\overline{\mu}_B}^\dagger|\Phi\rangle$$
$$+ \langle\Phi|\alpha_{\mu_B}\alpha_{\overline{\mu}_B}\hat{O}\alpha_{\overline{\mu}_B}^\dagger\alpha_{\mu_B}^\dagger|\Phi\rangle\big), \quad (13)$$

can also be written in a more compact form as

$$\langle\hat{O}\rangle_{\text{EFA}} = \tfrac{1}{2}\big(\langle\Phi|\alpha_{\mu_B}\hat{O}\alpha_{\mu_B}^\dagger|\Phi\rangle + \langle\Phi|\alpha_{\overline{\mu}_B}\hat{O}\alpha_{\overline{\mu}_B}^\dagger|\Phi\rangle\big)$$
$$= \tfrac{1}{2}\big(\langle\Phi|\hat{O}|\Phi\rangle + \langle\Phi|\alpha_{\mu_B}\alpha_{\overline{\mu}_B}\hat{O}\alpha_{\overline{\mu}_B}^\dagger\alpha_{\mu_B}^\dagger|\Phi\rangle\big). \quad (14)$$

This allows us to write the density matrix and pairing tensor as an average over one-quasiparticle excitations,

$$\rho_{kk'}^{\text{EFA}} = \tfrac{1}{2}\big(\langle\Phi|\alpha_{\mu_B}c_{k'}^\dagger c_k \alpha_{\mu_B}^\dagger|\Phi\rangle + \langle\Phi|\alpha_{\overline{\mu}_B}c_{k'}^\dagger c_k \alpha_{\overline{\mu}_B}^\dagger|\Phi\rangle\big) \quad (15)$$

and

$$\kappa_{kk'}^{\text{EFA}} = \tfrac{1}{2}\big(\langle\Phi|\alpha_{\mu_B}c_{k'} c_k \alpha_{\mu_B}^\dagger|\Phi\rangle + \langle\Phi|\alpha_{\overline{\mu}_B}c_{k'} c_k \alpha_{\overline{\mu}_B}^\dagger|\Phi\rangle\big), \quad (16)$$

which is a very intuitive result according to the expressions of Eqs. (4) and (5). This result, however, does by no means imply that the energy, which is the average of a two-body operator, could be written as $\tfrac{1}{2}(\langle\Phi|\alpha_{\mu_B}H\alpha_{\mu_B}^\dagger|\Phi\rangle + \langle\Phi|\alpha_{\overline{\mu}_B}H\alpha_{\overline{\mu}_B}^\dagger|\Phi\rangle)$.

Once the EFA energy is defined in terms of the density matrix and the pairing tensor, and those objects in terms of the Bogoliubov U and V amplitudes of Eq. (1), the application of the variational principle is straightforward, and it has been discussed at length in [8]. As in the case of other density functionals (Gogny, Skyrme, etc.) the rearrangement terms coming from the derivatives of the density are taken into account in the HFB equation. This is also the case for the BCPM calculations for even-even nuclei.

For higher order excitations including two, three, etc. quasiparticle excitations, one can proceed along the same lines as discussed above. For multiquasiparticle excitations the density matrix of Eq. (2) becomes

$$\rho_{kk'}^{(\mu_{B_1},...,\mu_{B_N})} = \langle\Phi|\bigg(\prod_\sigma \beta_\sigma\bigg)c_{k'}^\dagger c_k \bigg(\prod_\sigma \beta_\sigma^\dagger\bigg)|\Phi\rangle$$
$$= (V^*V^T)_{kk'} + \sum_\sigma (U_{k'\sigma}^* U_{k\sigma} - V_{k'\sigma}V_{k\sigma}^*), \quad (17)$$

where the index σ runs over the set $\mu_{B_1},\ldots,\mu_{B_N}$ for a N-quasiparticle excitation. With respect to the one-quasiparticle case, it amounts to replacing the term in parenthesis on the right-hand side of Eq. (2) by the sum on the right-hand side of Eq. (17). The corresponding expression for the κ pairing tensor can be easily obtained from Eq. (3).

The EFA expression for the multiquasiparticle excitation density is obtained from Eq. (17) by multiplying the sum on the right-hand side by one-half and extending the sum on the label σ to include the time-reverse quantum numbers of the

set $\mu_{B_1}, \ldots, \mu_{B_N}$. The same consideration applies straightforwardly to the EFA pairing tensor. The EFA density matrix and pairing tensors can be obtained from Eq. (9) by introducing the statistical probabilities

$$p_\sigma = \begin{cases} 1 & \sigma \in \mu_{B_1}, \ldots, \mu_{B_N} \text{ or } \in \overline{\mu}_{B_1}, \ldots, \overline{\mu}_{B_N}, \\ 0 & \text{otherwise.} \end{cases} \quad (18)$$

For instance, in the two-quasiparticle case, and according to Eq. (13) the EFA energy is the sum of multiple terms, most of them differing by mere permutations of the labels. Once this multiplicity is taken into account, one obtains

$$\begin{aligned} E_{\text{EFA}} = \tfrac{1}{16}(&\bullet + \mu \bullet \mu + \nu \bullet \nu + \overline{\mu} \bullet \overline{\mu} + \overline{\nu} \bullet \overline{\nu} \\ &+ \mu\nu \bullet \nu\mu + \mu\overline{\mu} \bullet \overline{\mu}\mu + \nu\overline{\nu} \bullet \overline{\nu}\nu \\ &+ \mu\overline{\nu} \bullet \overline{\nu}\mu + \nu\overline{\mu} \bullet \overline{\mu}\nu + \mu\nu \bullet \overline{\nu\mu} \\ &+ \mu\overline{\mu}\nu \bullet \nu\overline{\mu}\mu + \mu\overline{\mu\nu} \bullet \overline{\nu\mu}\mu + \mu\nu\overline{\nu} \bullet \overline{\nu}\nu\mu \\ &+ \overline{\mu}\nu\overline{\nu} \bullet \overline{\nu}\nu\overline{\mu} + \mu\overline{\mu}\nu\overline{\nu} \bullet \overline{\nu}\nu\overline{\mu}\mu), \end{aligned} \quad (19)$$

where, in order to simplify the expression, we have introduced an obvious notation. For instance, the term $\nu \bullet \nu$ represents the overlap $\langle \Phi | \beta_{\nu_B} \hat{H} \beta_{\nu_B}^\dagger | \Phi \rangle$. The average contains 16 terms. Moreover, the average is manifestly invariant under time reversal. As in the one-quasiparticle case, the average contains contributions from even and odd number parity states. In order to understand the contents of the previous average, it is convenient to use the quasiparticle representation of the Hamiltonian (see Appendix E of [26]) with the quasiparticle operators defined in such a way as to render the $H^{11} = \sum_\sigma E_\sigma \beta_\sigma^\dagger \beta_\sigma$ term diagonal. Using this representation, Eq. (19) becomes

$$E_{\text{EFA}} = \langle \Phi | \hat{H} | \Phi \rangle + \tfrac{1}{2}\left(E_{\mu_B} + E_{\overline{\mu}_B} + E_{\nu_B} + E_{\overline{\nu}_B} \right) + \cdots, \quad (20)$$

where the missing terms are contractions of the H^{22} part of the Hamiltonian.

A. The BCPM functional

The BCPM functional was proposed in Ref. [19] as an evolution of the BCP functional [32,33] to include several improvements aimed to reduce the original number of adjustable parameters. The idea was to use state-of-the-art microscopic nuclear matter calculations with realistic nuclear forces to obtain a realistic equation of state as a function of the density. To convert the numerical tables into some analytical form, a polynomial fit up to fifth order was used to fit the equation of state up to six times saturation density [32]. The same two polynomials (one for pure nuclear matter, the other for neutron matter) are used in finite nuclei replacing nuclear matter densities by the densities of finite nuclei. The functional is supplemented with a Gaussian term in the direct channel to simulate surface effects, a spin-orbit term with the same functional form as the Skyrme or Gogny interactions, the Coulomb potential among protons, and a density-dependent pairing term; see the recent review [24] for a more detailed explanation of the properties of BCPM and its application to nuclear structure problems [20,21,34–36] and astrophysics [22,23]. As mentioned in the introduction, the main deficiency of BCPM is the lack of time-odd densities, preventing

its use in those situations requiring the breaking of time-reversal invariance. Therefore, high spin physics, odd-mass systems, or multiquasiparticle excitations cannot be treated in the framework of BCPM. However, the fact that the EFA and full blocking provide similar results in calculations with Skyrme interactions suggests that the EFA can be used along with BCPM to define a functional for odd-mass systems or quasiparticle excitations. Based on the results with Skyrme and a comparison with Gogny forces described below, one can expect that the differences between the results obtained in the present approach and those obtained in a full blown blocking procedure are not going to be relevant in terms of the physics to be described.

B. Orthogonality

The variational character of the EFA is advantageous in many instances, but it also presents disadvantages in other aspects of the calculation. It is usually found in real calculations that most of the blocked configurations end up converging to the lowest energy configuration with the same set of quantum numbers. The only situation when this is no longer the case is when the initial blocked configuration has deformation parameters very different from the ones of the lowest energy solution, and therefore the iterative process starts in the neighborhood of a local minimum that cannot be avoided by the gradient method. This unwanted property implies that in a calculation breaking all symmetries it is very likely that only one blocked configuration is going to be reached, irrespective of the initial blocking configuration. This drawback of the method can be circumvented by introducing orthogonality constraints in the calculation [37]. However, it is easier and usually provides more physics insight to preserve axial symmetry in order to have K (the component of angular momentum along the third axis) as a good quantum number. In this way, orthogonality among different K values is automatic and therefore one is guaranteed at least one solution for each possible value of K. Additionally, if octupole deformation is not relevant, it is very likely that parity is also going to be preserved, giving two states for each K value.

In the results discussed below, axial symmetry is preserved and K is a good quantum number. Reflection symmetry is allowed to break but in many instances the solution preserves this symmetry to a large extent and therefore parity can be used as an "approximate" quantum number (the mean value of parity is computed and taking as a good quantum number if its absolute value is above 0.9). On the other hand, the orthogonality constraint is well defined in full blocking calculations and it has been implemented in all the examples considered. This is not the case with the EFA as the concept of orthogonality in a statistical ensemble is not well defined.

III. EFA VERSUS FULL BLOCKING

The equivalence between EFA and full blocking calculations has been empirically tested only in Skyrme forces [12]. It is the purpose of this section to extend the validity of the equivalence also to Gogny forces by presenting results obtained in both approaches with Gogny D1M for some selected
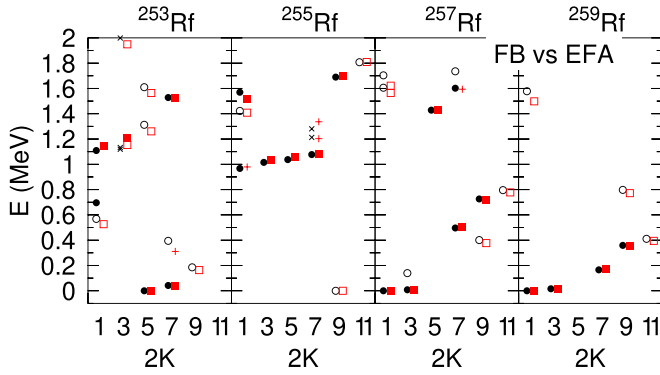
FIG. 1. The lowest energy excitation spectra for several rutherfordium isotopes computed with the Gogny D1M force, using full blocking and the EFA method. Each state is represented by a symbol according to its parity and the method employed for its calculation. Symbols are placed along the horizontal axis according to the value of $2K$. Filled (empty) black circles represent full blocking results with positive (negative) parity. States with octupole deformation and no definite parity are depicted with a black $\times$ symbol. Filled (empty) red squares are used for positive (negative) states obtained with EFA. States with octupole deformation and no definite parity are depicted with a red $+$ symbol. All symbols are slightly displaced along the horizontal axis to improve legibility.
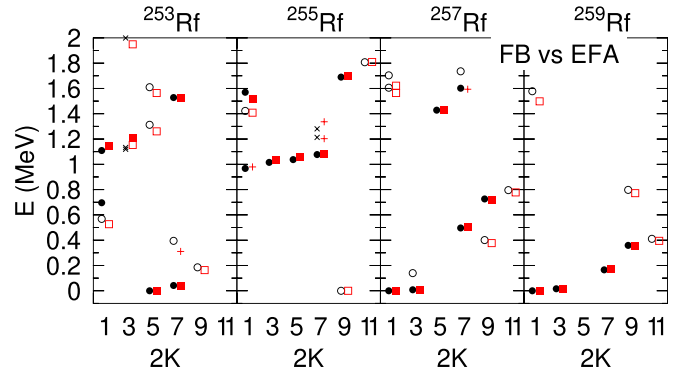

FIG. 2. A comparison of results obtained for Rf isotopes with full blocking and the Gogny force with D1S and D1M parametrizations. For an interpretation of the plot, see caption of Fig. 1. In the present case, black circles (red squares) represent D1S (D1M) calculations.

set of nuclei, the same used in the next section to empirically demonstrate the convenience of using EFA to describe odd-mass nuclei in BCPM. The choice of the Gogny force is not accidental and is based on its good pairing properties as well as its good description of high-spin physics [38], that critically relies on appropriate time-odd component of the force and pairing properties. For the full blocking calculation with the Gogny force, we use the results of Refs. [39,40]. For auxiliary HFB calculations for even-even systems we follow [41]. For other examples of EFA calculations with the Gogny force see [9,13,14,17,42,43].

In Fig. 1 a comparison of the results obtained with the Gogny D1M using full blocking and the EFA is shown for $^{253-259}$Rf isotopes. As can be clearly noticed, the correspondence between the EFA and full blocking results is one to one and remarkable. These results go along the conclusions of [12] for Skyrme forces and confirm the nearly perfect equivalence between EFA and full blocking in terms of excitation energies. All the levels have prolate quadrupole deformation with $\beta_2 \approx 0.28$ and negligible (except in some specific levels) octupole deformation. Please note that some levels obtained with full blocking do not have their counterpart in the EFA calculation. This is because in the EFA the orthogonality constraint has not been imposed.

It is also interesting to consider the different results obtained with different parametrizations of the Gogny force. It is well known in the literature that the excitation energy of different excited states in odd-mass nuclei is spread over a broad range of values depending on the force/functional used [14,15,42–44]. In Fig. 2 we compare our results with full blocking for D1S and D1M and the rutherfordium isotopes discussed above. In line with previous findings, we observe some dispersion in the excitation energies that is most likely

caused by slight changes in the position of the underlying single-particle levels or slightly different pairing correlations. It is clear that reaching the so-called spectroscopic accuracy (in the present context meaning perfect matching of spectra using different interactions) with forces containing 14 parameters, most of them adjusted to nuclear matter properties and aimed to be valid across the nuclear chart, is unfeasible. Spectroscopic accuracy can only be achieved by means of interactions fitted to very specific regions of the nuclear chart, as is customary in shell model calculations.

In Fig. 3 results obtained with the Gogny D1M using full blocking are compared to the EFA ones for plutonium, dysprosium and lanthanum isotopes. As in the rutherfordium case, the agreement is very good. Plutonium isotopes have a quadrupole deformation parameter $\beta_2 \approx 0.27$ in both the full blocking and EFA cases. Some of the levels obtained with full blocking have octupole deformation with β_3 as large as 0.1 in ^{239}Pu. In dysprosium isotopes, the deformation goes from $\beta_2 \approx 0.20$ in ^{155}Dy up to $\beta_2 \approx 0.30$ in ^{161}Dy. Octupole deformation is negligible in all the instances, being slightly larger in the EFA. In the odd-proton set of lanthanum isotopes, there is shape coexistence in ^{135}La with minima located at $\beta_2 \approx 0.10$ in the prolate side, and $\beta_2 \approx -0.10$ in the oblate one. The two isotopes $^{137-139}$La are spherical, whereas $\beta_2 \approx 0.06$ in ^{141}La. Again, octupole deformation is negligible. In the EFA case, ^{135}La and ^{141}La are slightly prolate with $\beta_2 \approx 0.12$ and $\beta_2 \approx 0.07$, respectively. As in the full blocking case, $^{137-139}$La are spherical.

IV. BCPM EFA

When the BCPM functional was postulated [19], similitude was noted between the results of Gogny D1M and those of BCPM for low energy nuclear structure quantities [20]. Therefore, it seems reasonable to compare the BCPM-EFA predictions for odd-A nuclei with Gogny D1M ones. The choice of D1M is further justified by its good performance in describing time-odd physics like rotational bands or odd-mass nuclei. In the following, we consider five different isotopic chains covering different regions of the nuclear chart: the superheavy element rutherfordium, the actinide plutonium, the
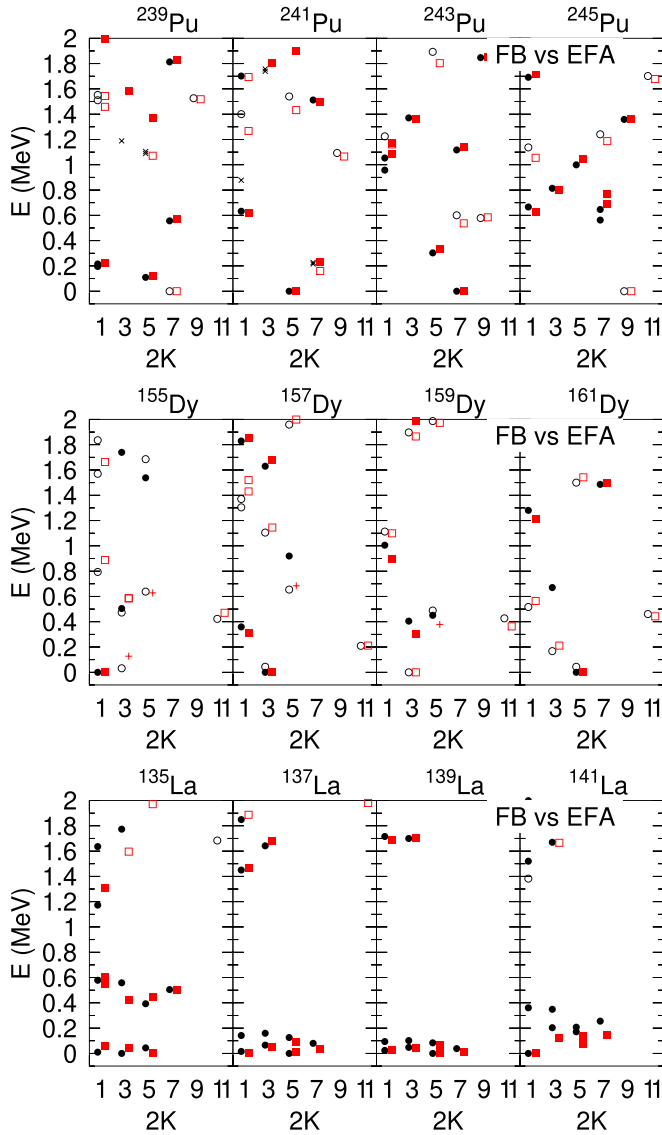
FIG. 3. A comparison of full blocking and EFA results for selected Pu, Dy, and La isotopes. For an interpretation of the plot, see caption of Fig. 1.

FIG. 4. The lowest energy spectrum obtained for $^{253-259}$Rf with the BCPM functional and the D1M Gogny force. For an interpretation of the plot, see caption of Fig. 1. In the present case, black circles (red squares) represent BCPM (D1M) calculations. Experimental ground state J values are marked with a gray bar. The height of the bar represents the energy window for the comparison with theoretical results (see text for details).

rare-earth elements lanthanum and dysprosium, and the light krypton isotopes. Overall, these five isotopic chains cover a large variety of nuclear deformations and mass numbers, providing a complete benchmark for BCPM-EFA calculations.

Regarding the comparison of the obtained spectra with experimental data, it has to be taken into account that there are many missing effects that could influence, to the level of a few hundred keV, the excitation energies obtained by the mean field, particle-vibration coupling being a common suspect [44]. Other factors that could influence the position of the levels are the correlation energies associated to various symmetry restorations [45], like particle number or angular momentum and parity, that depend on the detailed deformation and pairing properties of the levels. It is to be expected that the large rotational energy correction (of the order of a few MeV in the present case) can be slightly different for different orbitals (pairing correlations are different for each
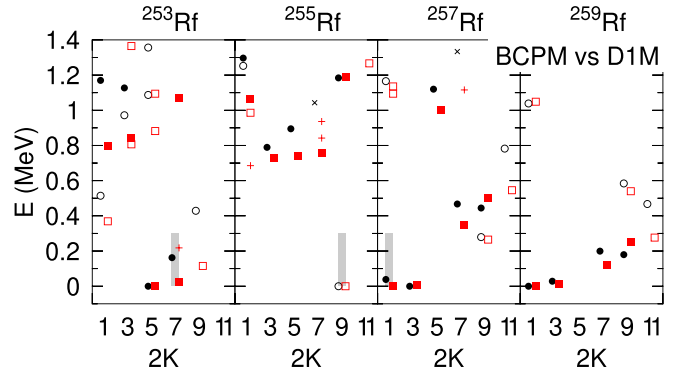
orbital and, accordingly, moments of inertia would also be different). The same argument applies to the zero-point energy correction associated with particle number restoration. Last but not least, correlation energies associated to fluctuations in the collective degrees of freedom (closely related to the particle-vibration coupling) are also expected to differ from one orbital to another. A substantial reshuffling of orbitals may occur after all these corrections have been implemented. Those unaccounted effects can modify the ordering of level with respect to the plain mean field results. Even though this is an exciting field of research and work along these lines is already in progress, it goes beyond the purpose of this work. We follow therefore a more pragmatic approach in the comparison with experimental data, and consider that calculations properly reproduce the experimental data if the predicted level lies within a window centered at the experimental value. In this work, we take an empirical width of 300 keV for such energy window.

A. Rutherfordium isotopes

In Fig. 4, the lowest-energy spectra obtained with BCPM and D1M for $^{253-259}$Rf isotopes are plotted. Please note that excitation energies of D1M have been multiplied by a factor 0.75 to compare with those of BCPM due to different effective masses (0.75 for D1M, 1.0 for BCPM). By looking at the spectra one can easily recognize the close similitude between the two calculations. There are some differences that can be attributed to specific positions of single-particle levels, but they are minor and usually do not alter the ordering of the different states. The β_2 deformation parameters of all the levels shown belong to the interval 0.27–0.29 for $^{253-257}$Rf and to the interval 0.26–0.28 for ^{259}Rf. In most cases, the β_3 octupole deformation parameter is zero and therefore parity is a good quantum number.

In both cases the excitation energy reduction with respect to the unperturbed one quasiparticle energy is a consequence of the quenching of pairing correlations due to the
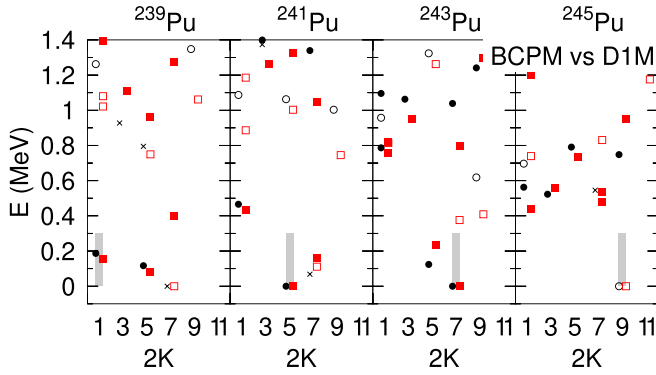
FIG. 5. The lowest energy spectrum obtained for $^{239-245}$Pu with the BCPM functional and the D1M Gogny force. For an interpretation of the plot, see caption of Fig. 1. In the present case, black circles (red squares) represent BCPM (D1M) calculations. Experimental ground state J values are marked with a gray bar. The height of the bar represents the energy window for the comparison with theoretical results (see text for details).

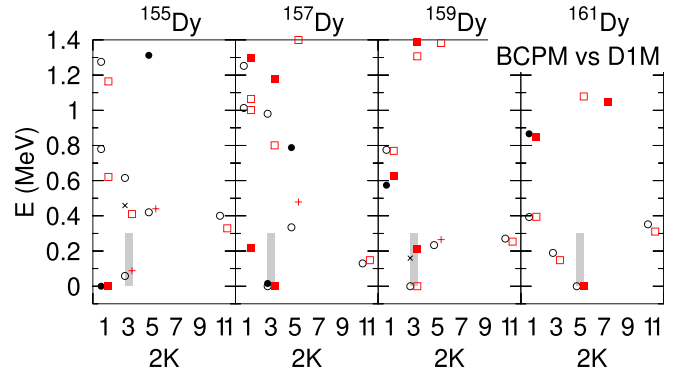
FIG. 6. The lowest energy spectrum obtained for $^{155-161}$Dy with the BCPM functional and the D1M Gogny force. For an interpretation of the plot, see caption of Fig. 1. In the present case, black circles (red squares) represent BCPM (D1M) calculations. Experimental ground state J values are marked with a gray bar. The height of the bar represents the energy window for the comparison with theoretical results (see text for details).

"pseudoblocking" effect of EFA. A measure of pairing correlation strength is the particle-particle energy $\text{Tr}(\Delta\kappa)/2$. In the present case, while the proton p-p energy remains more or less the same as the one of the neighbor even-even isotopes, it is quenched by a factor of around 2 in the neutron channel. The quenching factor can reach a value of four in some cases, like the $7/2^+$ state in ^{253}Rf. Also, pairing correlations in the neutron channel can disappear as in the case of the $9/2^-$ in ^{255}Rf. This result indicates that binding energies obtained within the EFA framework may substantially differ from those from perturbative schemes [5,7] often used in large scale calculations.

Experimental data in this region is scarce [46], and all the spin and parity assignments are tentative. The isotope ^{253}Rf has a tentative $7/2^+$ ground state that could correspond to the predicted $7/2^+$ observed at around 200 keV excitation energy in Fig. 4. ^{255}Rf has a tentative $9/2^-$ experimental ground state in agreement with both predictions. For ^{257}Rf, the lowest states are $1/2^+$, $5/2^+$, and $11/2^-$. In our calculations those levels appear at an excitation energy of 20, 1120, and 794 keV, respectively. For the isotope ^{259}Rf there are no experimental data available. In light of these results we conclude that, despite the absence of beyond mean-field effects discussed above, the agreement with experimental data is satisfactory.

B. Plutonium isotopes

Results for plutonium isotopes corresponding to mass numbers $A = 239$–245 are shown in Fig. 5 for both BCPM and Gogny D1M. As in the previous case, we find a close similitude in both spectra. The experimental ground-state angular momentum and parity taken from Ref [46] are $J^\pi = 1/2^+$, $J^\pi = 5/2^+ J^\pi = 7/2^+$, and $J^\pi = 9/2^-$, respectively. Those values are accurately predicted by both EDFs, with the exception of $J^\pi = 1/2^+$ in ^{239}Pu, that appears in the calculations at an excitation energy of around 100 keV (which is within the 300 keV window discussed above). The ground state has a β_2 deformation of 0.27 in the three cases and shows

no trace of reflection asymmetry. For the lighter $^{229-237}$Pu isotopes, all the experimental ground-state J^π values [46] are predicted by BCPM within the 300 keV energy window. The only exception is for the $J^\pi = 7/2^-$ ground state in ^{237}Pu, which lies at 0.530 MeV excitation energy with BCPM.

C. Dysprosium isotopic chain

Results for the $^{155-161}$Dy isotopes are displayed in Fig. 6. The four isotopes are prolate, with β_2 ranging from 0.23 in ^{155}Dy to 0.32 in ^{161}Dy. Each of the levels displayed in Fig. 6 has its own β_2 deformation, that differs by ± 0.04 from the quadrupole deformation of the ground state. As in the previous cases, the agreement between BCPM and D1M results is remarkable. In the four isotopes $^{155-161}$Dy there is a known isomeric state [46] with $J^\pi = 11/2^-$ at excitation energies of 234, 199, 352, and 485 keV, respectively. This isomeric state is well reproduced by the calculations. In ^{157}Dy there is an additional isomeric state, $J^\pi = 9/2^+$ at 162 keV, that is not observed in our calculations. Spin and parity of the ground state is known experimentally for the isotopes $^{139-171}$Dy [46]. Of those, BCPM reproduces the correct J^π value in six isotopes (35%), and in another four (24%) the corresponding excited state lies below 300 keV. The quadrupole deformation of the isotopes obtained in the BCPM calculation is mostly prolate but there is a region of oblate ground state in $^{141-153}$Dy.

D. Lanthanum isotopic chain

As an example of odd-Z isotopes, we calculate the low-lying spectra of lanthanum isotopes. For the odd-A lanthanum isotopes, there are known 13 values of the ground-state spin and parity, corresponding to $^{125-149}$La [46]. The results of our calculations agree with the experiment in four occasions (31%). This success rate is consistent with the hit rate obtained with other EDF approaches [7,44]. If one includes as hits in the comparison with experiment those states which in the calculation appear at an excitation energy lower than 300 keV,
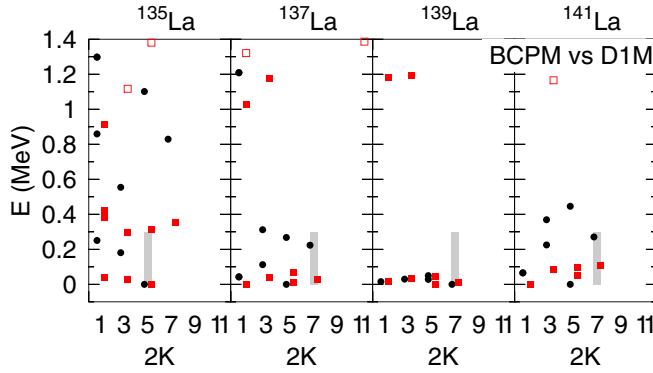
FIG. 7. The lowest energy spectrum obtained for $^{135-141}$La with the BCPM functional and the D1M Gogny force using the EFA. For an interpretation of the plot, see caption of Fig. 1. In the present case, black circles (red squares) represent BCPM (D1M) calculations. Experimental ground state J values are marked with a gray bar. The height of the bar represents the energy window for the comparison with theoretical results (see text for details).
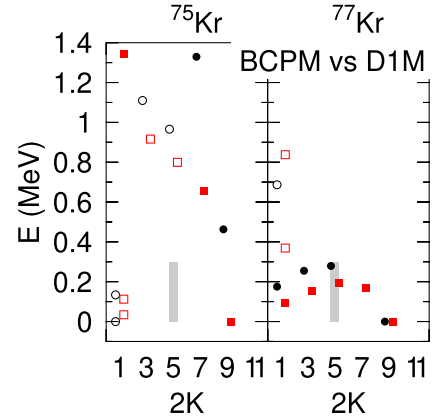

FIG. 8. The lowest energy spectrum obtained for ^{75,77}Kr with the BCPM functional (a) and the D1M Gogny force (b) using the EFA. For an interpretation of the plot, see caption of Fig. 1. In the present case, black circles (red squares) represent BCPM (D1M) calculations. Experimental ground state J values are marked with a gray bar. The height of the bar represents the energy window for the comparison with theoretical results (see text for details).

the number of J^π values in agreement goes up to ten (77% success). Of the remaining three cases, two correspond to light proton-rich isotopes, and the third to ^{143}La. The latter case deserves further theoretical studies considering fluctuations in relevant collective degrees of freedom in order to understand the discrepancy. The range of isotopes compared include prolate, deformed, and spherical nuclei. We point out that ^{145}La and ^{147}La, with neutron numbers close to the "octupole magic number" $N = 88$, are octupole deformed with $\beta_3 \approx 0.1$. The isotope ^{149}La is also octupole deformed, but with a slightly smaller β_3 around 0.05. However, the depths of the octupole well are only 150, 100, and 10 keV for ^{145}La, ^{147}La, and ^{149}La, respectively, which are not large enough to speak about permanent octupole deformation. Given that octupole depth wells tend to become deeper at high spins, it is possible for these nuclei to develop alternating parity rotational bands.

In Fig. 7, we show the lowest-energy spectra of $^{135-141}$La isotopes. There are a bunch of almost degenerate levels in ^{139}La for BCPM and in $^{137-139}$La for D1M, consequence of a low quadrupole deformation compatible with spherical nuclei. Those levels could be assigned to a spherical $J^\pi = 7/2^+$ ground state in agreement with experimental data. In the remaining isotopes deformation breaks the degeneracy but still experimental data are reproduced.

E. Kripton isotopes

Finally, we consider two krypton isotopes as an example of nuclei in the low mass region of the nuclear chart. The description of these nuclei is very challenging as it is well known that prolate-oblate (and triaxial) configurations coexist in a narrow range of energies close to the ground state. Therefore, one can consider this comparison as a worst case scenario, and expect a degradation in the comparison between BCPM and D1M with respect to the examples discussed in the previous sections. In Fig. 8 we show the spectra of ^{75,77}Kr for the two considered interactions. The different levels show different values of deformation. For instance, in ^{75}Kr with

the BCPM EDF, the β_2 deformation parameters of the five lowest states are 0.01, -0.05, 0.00, -0.15, and 0.04. This alternation of spherical, oblate and prolate states is a clear indication of shape coexistence. For the same nucleus but with D1M, there is a clear dominance of oblate deformations with deformation parameters as large as $\beta_2 = -0.2$, in agreement with the deeper oblate well obtained with D1M. For ^{77}Kr, the deformation obtained with BCPM is almost spherical, whereas for D1M it is oblate (but not as large as in ^{75}Kr). Experimental values for the ground state are $J^\pi = 5/2^+$ in both cases. The comparison with calculation results is not bad for ^{77}Kr but this is not the case for ^{75}Kr. The differences in deformation discussed above explain the larger discrepancies between BCPM, D1M, and experiment found in the present case.

F. Multiquasiparticle excitations

The study and discussion of multiquasiparticle excitations in atomic nuclei is a complex issue that deserves a separate publication. In this paper, we will just show an example of results obtained for high-K excitations in ^{178}Hf with EFA-BCPM, and compare them with the homologous results obtained with the D1S and D1M Gogny parametrizations. The choice of high-K isomers is not arbitrary, as these states are easier to identify experimentally and less prone to orthogonality issues. In Fig. 9 the results of EFA calculations for high-K isomeric states in ^{178}Hf are shown along with experimental data. There are five known high-K isomers in this nucleus. The 6^+ is assigned to a two-quasiparticle proton excitation, like one of the 8^- state. The other 8^- is a two-neutron quasiparticle excitation. Finally, both the 14^- and 16^+ states are four-quasiparticle excitations composed of a two-proton excitation along with a two-neutron one. One observes consistency among the theoretical results as well as a good agreement with experimental data. This example shows
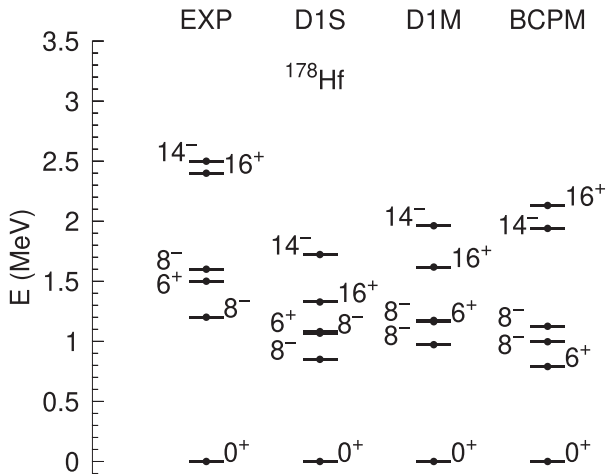
FIG. 9. High-*K* states in ^{178}Hf obtained with the EFA using BCPM, Gogny D1S and Gogny D1M are compared with experimental data. The Gogny excitation energies have been compressed by a factor 0.75 to account for the effective mass.

that the EFA-BCPM provides a suitable description of two- and four-quasiparticle excitations.

V. CONCLUSIONS

We implement the equal filling approximation (EFA) with the BCPM energy density functional, opening up the calculation of nuclei with an odd number of protons and/or neutrons. We first test the equivalence between EFA and full blocking calculations by studying the low-energy spectra predicted by the Gogny D1S and D1M interaction. We then compare the EFA BCPM predictions with the D1M ones along several isotopic chains. Once the normalization due to the effective

mass is taken into account, we find that the energy spectra predicted by the two interactions show a remarkable similarity, with most of the energy levels agreeing within 200 keV. We conclude therefore that BCPM and D1M have a similar quality in describing nuclear low-energy spectra across the nuclear chart. We observe a general quenching of pairing correlations due to the EFA "pseudoblocking" effect, which reduces the excitation energy with respect to the unperturbed one-quasiparticle energy. This result suggests that odd-even staggering in perturbative calculations could be sensibly reduced in the EFA scheme. We then performed a comparison with experimental data for ground state J^{π} values, and find that BCPM can reproduce most of the data within an energy window of 300 keV. Given the impact of many-body effects beyond mean-field affecting the nuclear spectrum (such as particle-vibration coupling, symmetry restoration effects, etc.), we consider the agreement satisfactory, also taking into account that effective interactions with just a few (tens of) parameters are not able to capture the full nuclear dynamics across the whole nuclear chart. Finally, two- and four-quasiparticle excitations are studied by looking at high-*K* isomers in ^{178}Hf. A close resemblance between BCPM, D1S and D1M predictions is found, with a sensible reproduction of experimental data. These results open the door to use BCPM for large scale calculations involving odd-*A* and/or multiquasiparticle excitations.

[1] K. Rutz, M. Bender, P.-G. Reinhard, J. Maruhn, and W. Greiner, Nucl. Phys. A **634**, 67 (1998).

[2] K. Rutz, M. Bender, P.-G. Reinhard, and J. A. Maruhn, Phys. Lett. B **468**, 1 (1999).

[3] S. Ćwiok, W. Nazarewicz, and P. H. Heenen, Phys. Rev. Lett. **83**, 1108 (1999).

[4] M. Bender, K. Rutz, P. G. Reinhard, and J. A. Maruhn, Eur. Phys. J. A **8**, 59 (2000).

[5] T. Duguet, P. Bonche, P.-H. Heenen, and J. Meyer, Phys. Rev. C **65**, 014310 (2001).

[6] T. Duguet, P. Bonche, P.-H. Heenen, and J. Meyer, Phys. Rev. C **65**, 014311 (2001).

[7] L. Bonneau, P. Quentin, and P. Möller, Phys. Rev. C **76**, 024320 (2007).

[8] S. Perez-Martin and L. M. Robledo, Phys. Rev. C **78**, 014304 (2008).

[9] S. Perez-Martin and L. M. Robledo, Int. J. Mod. Phys. E **18**, 788 (2009).

[10] G. Bertsch, J. Dobaczewski, W. Nazarewicz, and J. Pei, Phys. Rev. A **79**, 043602 (2009).

[11] A. V. Afanasjev and H. Abusara, Phys. Rev. C **81**, 014309 (2010).

[12] N. Schunck, J. Dobaczewski, J. McDonnell, J. Moré, W. Nazarewicz, J. Sarich, and M. V. Stoitsov, Phys. Rev. C **81**, 024316 (2010).

[13] R. Rodriguez-Guzman, P. Sarriguren, and L. M. Robledo, Phys. Rev. C **82**, 044318 (2010).

[14] R. Rodriguez-Guzman, P. Sarriguren, and L. M. Robledo, Phys. Rev. C **82**, 061302(R) (2010).

[15] J. Dobaczewski, A. V. Afanasjev, M. Bender, L. M. Robledo, and Y. Shi, Nucl. Phys. A **944**, 388 (2015).

[16] R. Rodríguez-Guzmán and L. M. Robledo, Eur. Phys. J. A **52**, 348 (2016).

[17] R. Rodrıguez-Guzmán and L. M. Robledo, Eur. Phys. J. A **53**, 245 (2017).

[18] W. Ryssens, G. Scamps, S. Goriely, and M. Bender, Eur. Phys. J. A **58**, 246 (2022).

[19] M. Baldo, L. M. Robledo, P. Schuck, and X. Viñas, Phys. Rev. C **87**, 064305 (2013).

[20] S. A. Giuliani and L. M. Robledo, Phys. Rev. C **88**, 054325 (2013).

[21] S. A. Giuliani, G. Martínez-Pinedo, and L. M. Robledo, Phys. Rev. C **97**, 034323 (2018).

[22] S. A. Giuliani, G. Martínez-Pinedo, M.-R. Wu, and L. M. Robledo, Phys. Rev. C **102**, 045804 (2020).

[23] B. K. Sharma, M. Centelles, X. Viñas, M. Baldo, and G. F. Burgio, Astron. Astrophys. **584**, A103 (2015) .

[24] M. Baldo, L. M. Robledo, and X. Viñas, Eur. Phys. J. A **59**, 156 (2023).

[25] E. Garrido, P. Sarriguren, E. M. de Guerra, and P. Schuck, Phys. Rev. C **60**, 064312 (1999).

[26] P. Ring and P. Schuck, *The Nuclear Many Body Problem* (Springer, Berlin, 1980).

[27] J. von Delft, A. D. Zaikin, D. S. Golubev, and W. Tichy, Phys. Rev. Lett. **77**, 3189 (1996).

[28] R. Rossignoli, N. Canosa, and P. Ring, Phys. Rev. Lett. **80**, 1853 (1998).

[29] K. Esashika, H. Nakada, and K. Tanabe, Phys. Rev. C **72**, 044303 (2005).

[30] M. Gaudin, Nucl. Phys. **15**, 89 (1960).

[31] S. Perez-Martin and L. M. Robledo, Phys. Rev. C **76**, 064314 (2007).

[32] M. Baldo, P. Schuck, and X. Viñas, Phys. Lett. B **663**, 390 (2008).

[33] M. Baldo, L. Robledo, P. Schuck, and X. Viñas, J. Phys. G: Nucl. Phys. **37**, 064015 (2010).

[34] S. A. Giuliani, L. M. Robledo, and R. Rodríguez-Guzmán, Phys. Rev. C **90**, 054311 (2014).

[35] L. Neufcourt, Y. Cao, S. Giuliani, W. Nazarewicz, E. Olsen, and O. B. Tarasov, Phys. Rev. C **101**, 014319 (2020).

[36] L. Neufcourt, Y. Cao, S. A. Giuliani, W. Nazarewicz, E. Olsen, and O. B. Tarasov, Phys. Rev. C **101**, 044307 (2020).

[37] J. Egido, H.-J. Mang, and P. Ring, Nucl. Phys. A **334**, 1 (1980).

[38] L. M. Robledo, T. R. Rodríguez, and R. R. Rodríguez-Guzmán, J. Phys. G: Nucl. Part. Phys. **46**, 013001 (2019).

[39] L. M. Robledo, R. Bernard, and G. F. Bertsch, Phys. Rev. C **86**, 064313 (2012).

[40] L. M. Robledo, R. N. Bernard, and G. F. Bertsch, Phys. Rev. C **89**, 021303(R) (2014).

[41] L. M. Robledo and G. F. Bertsch, Phys. Rev. C **84**, 014312 (2011).

[42] R. Rodríguez-Guzmán, P. Sarriguren, L. Robledo, and S. Perez-Martin, Phys. Lett. B **691**, 202 (2010).

[43] R. Rodriguez-Guzman, P. Sarriguren, and L. M. Robledo, Phys. Rev. C **83**, 044307 (2011).

[44] A. Afanasjev and S. Shawaqfeh, Phys. Lett. B **706**, 177 (2011).

[45] J. A. Sheikh, J. Dobaczewski, P. Ring, L. M. Robledo, and C. Yannouleas, J. Phys. G: Nucl. Part. Phys. **48**, 123001 (2021).

[46] F. Kondev, M. Wang, W. Huang, S. Naimi, and G. Audi, Chin. Phys. C **45**, 030001 (2021).